Chapter 3
Symphyseal Fusion in Selenodont Artiodactyls: New Insights from In Vivo and Comparative Data

Susan H. Williams, Christine E. Wall, Christopher J. Vinyard, and William L. Hylander

Contents

3.1 Introduction

Comparative and in vivo studies in primates (e.g., Hylander, 1977, 1979a, b, 1984, 1985; Hylander and Johnson, 1994; Hylander et al., 1987, 2000; Luschei and Goodwin, 1974; Vinyard et al., 2001) have contributed significantly to our understanding of mammalian craniofacial biology and function. Hylander and colleagues, in particular, have amassed a unique data set, arguably unmatched in any clade of mammals, in their effort to elucidate form–function relationships in the

S.H. Williams
Department of Biomedical Sciences, Ohio University College of Osteopathic Medicine, Ohio University, Athens, OH 45701
e-mail: willias7@ohio.edu

C. Vinyard et al. (eds.), *Primate Craniofacial Function and Biology*,
DOI: 10.1007/978-0-387-76585-3_3,

primate masticatory apparatus. This data set consists of comparative biomechanical analyses and in vivo mandibular bone strain and jaw-muscle electromyographic (EMG) recordings (e.g., Hylander, 1977, 1979a, b, 1984, 1985; Hylander and Johnson, 1994; Hylander et al., 1987, 2000, 2003, 2004). Many of these studies investigate suborder differences in primate jaw form, focusing on the functional and adaptive significance of the evolution of early ontogenetic ossification, or fusion, of the mandibular symphysis, a crown anthropoid synapomorphy.

One consistent finding of these studies is that jaw-muscle motor patterns during mastication differ between anthropoids and those strepsirrhines with a fully unfused and highly mobile symphyseal joint. Specifically, there is a strong correlation between the timing and magnitude of activity of the balancing-side deep masseter and symphyseal fusion. In vivo data from strepsirrhines, represented by galagos and ring-tailed lemurs, show that they typically recruit relatively low levels of activity from the balancing-side deep masseter *early* in the power stroke at a time when other jaw adductors are highly active and can resist the laterally directed pull of the balancing-side deep masseter (Hylander and Johnson, 1994; Hylander et al., 2002, 2004; Vinyard et al., 2006). In contrast, anthropoids, represented by macaques, baboons, owl monkeys, marmosets, and tamarins, show relatively high levels of recruitment from the balancing-side deep masseter *late* in the power stroke when most of the other jaw muscles are unloading (Hylander and Johnson, 1994; Hylander et al., 2003, 2004; Vinyard et al. 2001).

Simultaneous bone strain data from the labial surface of the macaque symphysis and jaw-muscle EMG data demonstrate the effect that this motor pattern has on symphyseal strains during routine mastication. Specifically, the transverse force generated by the pronounced activity of the balancing-side deep masseter is largely unresisted by the other jaw muscles because they are unloading. This causes the symphysis to be bent transversely, with the two dentaries being pulled apart laterally, as in a wishbone (Hylander, 1984, 1985; Hylander and Johnson, 1994; Hylander et al., 1987). During lateral transverse bending – or "wishboning" – of the symphysis, the bone along the labial aspect of the macaque symphysis is placed in compression while the bone along the lingual aspect is placed in tension. The magnitude of the tensile strains along the lingual aspect of the symphysis has been estimated by considering the symphysis as a curved beam loaded in its plane of bending. These estimates suggest that the lingual tensile strains will be more than 3.5 times the compressive strains along the labial aspect of the symphysis. Given the recorded compressive strains along the labial surface of the macaque symphysis, Hylander (1984, 1985; Hylander et al., 1987) estimated that the tensile strains along the lingual surface may routinely exceed 2,000 microstrain ($\mu\varepsilon$) during normal mastication.

Researchers have further proposed that symphyseal fusion coupled with the delayed and pronounced activity of the balancing-side deep masseter has an adaptive significance. Specifically, it may have enabled anthropoids to consume tougher and or harder foods that require additional and/or more forceful processing (Hylander, 1979a, b, 1984, 1985; Hylander et al., 2000; Ravosa, 1999; Ravosa and Hylander, 1994; Ravosa et al., 2000). Whereas, the delayed and pronounced activity of

the balancing-side deep masseter probably has the effect of generating increased transverse bite force and may also increase the length of the power stroke, fusion strengthens the symphysis to resist the resulting increased wishboning stresses and strains (Hylander, 1979a, b, 1984, 1985; Hylander et al., 2000; Ravosa, 1999; Ravosa and Hylander, 1994; Ravosa et al., 2000).

The significance of the link between masticatory loads and symphyseal fusion can be appreciated by considering the behavior of cortical bone when it is loaded. Cortical bone is weaker – i.e., it more readily yields and fails – in tension than in compression, and this is particularly true when it is subjected to cyclical loading (Carter et al., 1981; Keaveny and Hayes, 1993). When it is subjected to a single tensile load, it yields around 6,300 με, and the strain at which it yields and ultimately fails decreases with an increased number of loading cycles. For example, bone fails around 3,500 με after 850 cycles in tension and around 3,000 με after 1,000 loading cycles (Carter et al., 1977). Because fatigue failure of bone can occur under normal physiologic conditions, the remodeling process that repairs bone must outpace the accumulation of microscopic damage for bone to maintain its structural integrity. Alternatively, strain levels can remain below a critical level to avoid this microdamage. Given this mechanical response of bone to cyclical tensile loading, the strains recorded from the macaque symphysis, and associated muscle activation patterns, Hylander (1984) has suggested that critical strain levels may be around 3,000 με for animals that typically chew and wishbone their symphyses tens of thousands of times per day, as may be the case for many anthropoid folivores. In contrast, structural damage of the symphysis due to wishboning is likely not a significant issue for most unfused primates, because they appear to not have the delayed and/or pronounced activity of the balancing-side deep masseter (Hylander and Johnson 1994; Hylander et al., 2000).

While much of the in vivo and comparative work on symphyseal fusion focuses on anthropoid primates, these are not the only mammals to have evolved this derived morphology. For example, among selenodont artiodactyls, all camelids (e.g., alpacas, vicuñas, and camels) typically fuse their symphyses early during ontogeny. Moreover, according to Hogue and Ravosa (2001), they exhibit some of the same allometric scaling patterns of the mandible that would be beneficial for resisting wishboning. Both anthropoid and camelids have relatively anteroposteriorly elongate symphyses compared to strepsirrhines and non-camelids, respectively (Hogue and Ravosa, 2001; Ravosa, 1991; Ravosa and Hylander, 1994). Increasing the anteroposterior length of the symphysis is the most efficient way to increase the resistance of the symphysis against wishboning. This is because bending stresses in a beam are inversely proportional to the second moment of inertia (I) relative to the plane of bending, where $I = a^2b$, a equals the diameter in the plane of bending – or the anteroposterior length – and b equals the diameter perpendicular to a. Camelids also have relatively wider mandibular corpora than non-camelid selenodont artiodactyls (Hogue and Ravosa, 2001). Interestingly, symphyseal curvature, which may alter wishboning stresses along the lingual border of the symphysis, does not differ between these two groups. Thus, Hogue and Ravosa (2001) propose that wishboning and symphyseal fusion may be linked in camelids.

These comparative findings are supported by recent EMG studies in two species of selenodont artiodactyls – goats and alpacas. These studies show that alpacas have a wishboning jaw-adductor motor pattern like anthropoids. That is, they recruit their balancing-side deep masseter relatively late in the power stroke (Williams, 2004; Williams et al., 2003, 2007). In contrast to alpacas, goats and other non-camelid selenodont artiodactyls are similar to strepsirrhines in having mobile symphyses united by ligaments, fibrocartilage, and interdigitating bony rugosities (Lieberman and Crompton, 2000). As in many strepsirrhines, goats also recruit their balancing-side deep masseter relatively early in the power stroke (Fig. 3.1) (Williams, 2004; Williams et al., 2003, 2007). Thus, there is also strong association in selenodont artiodactyls between symphyseal fusion, symphyseal shapes advantageous for resisting wishboning, and the wishboning jaw-muscle activity pattern.

The combined comparative and in vivo evidence outlined above suggests that wishboning would be a predominant loading regime along the alpaca symphysis. If true, symphyseal fusion in camelids may have a similar adaptive significance as has been proposed for anthropoids. Here, we summarize symphyseal strain data from a series of experiments on alpacas (*Lama pacos*) to determine whether alpacas wishbone their symphyses.

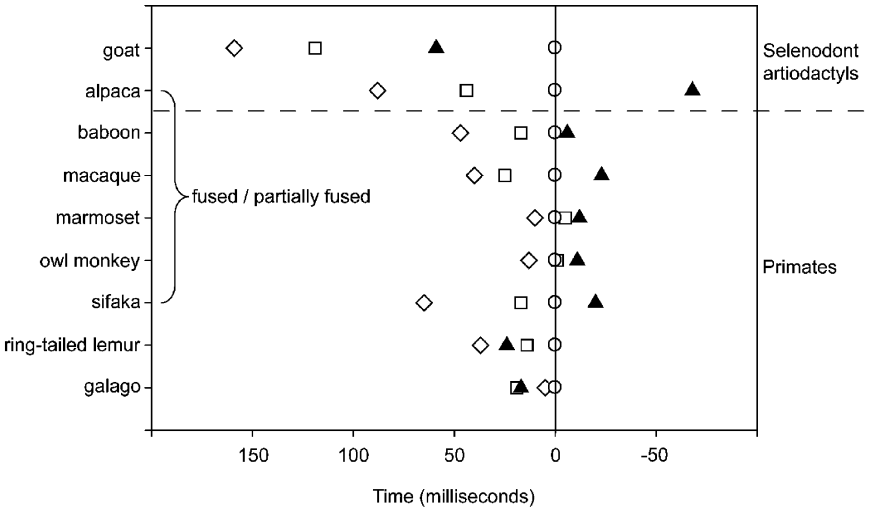

Fig. 3.1 Summary data of peak masseter activity in primates and selenodont artiodactyls. diamonds, working-side deep masseter; squares, balancing-side superficial masseter; triangles, balancing-side deep masseter; circles, working-side superficial masseter. The balancing-side deep masseter peaks later relative to other jaw muscles in species that fuse their symphyses early during ontogeny or have the tendency to develop partial fusion (e.g., sifakas). Primate data are from Hylander and Johnson (1994), Hylander et al. (1987, 2000, 2002, 2003, 2004), and Vinyard et al. (2001, 2006)

3.2 Methods

Three types of strain data from alpacas are presented in this paper: (1) in vitro symphyseal strains resulting from simulated stresses on a fresh cadaveric specimen; (2) in vivo symphyseal strains resulting from simulated stresses on anesthetized subjects; (3) in vivo symphyseal strains from alert individuals during normal mastication. The in vitro data set is useful for characterizing the expected strain patterns along the entire symphysis during simulated loading regimes, whereas the simulated stresses on live alpacas provide a baseline for interpreting the strains recorded from these same animals during mastication. Because these last two data sets are from the same gauges used for recording masticatory strains, methods for these data sets are discussed together.

3.2.1 In Vitro Stresses – Gauge Placement, Recording, and Analysis

Eight rectangular rosette strain gauges (WA-06-060WR-120, Micro-Measurements, Raleigh, NC) and single-element gauges (FRA-1-11-1L, Sokki Kenkyujo Co., Tokyo) were attached along the horizontally oriented labial and lingual surfaces of the symphysis of a fresh alpaca mandible harvested from a cadaveric specimen. Each rosette was placed along the midline of the symphysis with one element oriented perpendicular to the long axis of the symphysis. In the case of the rosettes, this was the B-element. A single-element gauge oriented similarly was also placed directly on the vertically oriented and curved lingual surface of the symphysis Fig. 3.2).

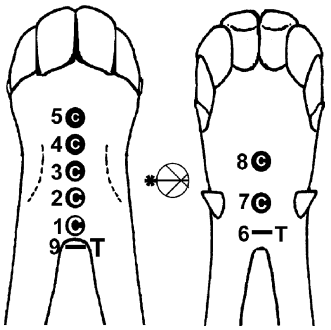

Fig. 3.2 Summary data of in vitro symphyseal strains along the labial (*left*) and lingual (*right*) surfaces of the alpaca symphysis during simulating lateral transverse bending, or wishboning. C, compression; T, tension. Numbers refer to gauges discussed in the text. Gauges 1–5 and 7–8 are rectangular rosettes and gauges 6 and 9 are single element gauges. The orientation of each rosette B-element and the single-element gauges is indicated by the *asterik*. Gauge 9 is attached to the symphysis directly on the curved, vertically oriented lingual surface. The strain gradient of tension or compression along the B- and single-elements is indicated by the letter size

Wishboning was simulated by pulling the two halves of the mandible apart at the level of the insertion of the deep masseter just below the mandibular notch. Reverse wishboning was simulated by pushing the two halves of the mandible together at this same level. The raw strain output for each element during simulated medial and lateral transverse bending – or reverse wishboning and wishboning, respectively – were recorded directly to paper via a Gould Brush 260 chart recorder. A calibration signal was also recorded to the chart recorder paper. The polarity and relative magnitude of the raw strains from each of the elements were determined from these chart recordings.

3.2.2 In Vivo Stresses – Gauge Placement, Recording, and Analysis

Symphyseal strain data were collected from four adult female alpacas. These animals were on loan from the Camelid Research Program of the College of Veterinary Medicine of Ohio State University. Prior to gauge placement, animals were fully anesthetized using an intramuscular injection of 5 mg/kg ketamine, 0.05–0.1 mg/kg butorphanol, 0.5 mg/kg xylazine (Mama, 2000). The skin over the symphysis was shaved and then infiltrated with a local anesthetic (lidocaine HCl) containing epinephrine (1:100,000). A small incision (< 2 cm) was made along the caudal border of the symphysis, and the skin and underlying periosteum reflected to expose the bone. The bone was then degreased and neutralized, and the gauge was attached to the bone using a cyanoacrylate adhesive. Delta rosettes (SA-06-030WY-120, Micro-Measurements, Raleigh, NC) were bonded in the midline on the labial surface of the symphysis, in the position of gauge 1 in Fig. 3.2. The A-element of the rosette was oriented parallel to the long axis of the symphysis. The incision was then sutured closed around the lead wires, which exited the incision and connected to the strain bridges.

Prior to the animal's recovery from anesthesia, the symphyses of two of the four alpacas (Alpacas 2 and 4) were gently reverse wishboned as described above. This was done to ensure that the gauges functioned properly and to facilitate the interpretation of the strain data recorded during mastication. Once fully alert and standing, the animals were fed hay. The resulting voltage output from each of the strain-gauge elements during the load simulations and mastication was conditioned and amplified (Vishay 2100 System, Vishay Instruments), and recorded at 15 in/s with a multiple-channel FM tape recorder (Honeywell 101e). Sequences were identified as left or right chews from an audio track on the tape recorder. Strain data were also monitored on a six-channel chart recorder (Gould Brush 260). In one experiment, (Alpaca 4 Experiment 2), a split screen of the subject and the strain tracings on the chart recorder was recorded to video using special effects generator so that bone strain could be qualitatively correlated with jaw movements. After sufficient data were collected, the animals were re-anesthetized and the gauges were removed. All recoveries were uneventful and the animals were administered

prophylactic doses of antibiotics (Dual-Cillin) the day of and for several days following the experiment.

The raw strain data from the simulated stress sequences and from selected sequences of vigorous rhythmic chewing were digitized at a sampling rate of 500 Hz and filtered with a digital Butterworth low-pass filter set at 40 Hz. The magnitude of the maximum and minimum principal strains (ε_1 and ε_2, respectively), shear strain (γmax), and the angular value of ε_1 (the angle Φ) were calculated over 2-ms intervals. γmax is calculated as ε_1–ε_2; because ε_1 is usually positive and ε_2 is usually negative, γmax is usually greater than both ε_1 and ε_2. The peak strains for each power stroke were identified as those coinciding with γmax. The angular value of ε_1 was measured relative to the long axis of the A-element of the delta-rosette strain gauge (and parallel to the long axis of the symphysis). Positive values were measured counterclockwise to the A-element and negative values were measured clockwise to the A-element. The angular value of ε_2 is always at $\pm 90^\circ$ to the angular value of ε_1.

Descriptive statistics of ε_1, ε_2, $\varepsilon_1/\varepsilon_2$ and the direction of ε_1 were calculated at γmax and for the 25% levels of peak γmax along the mandibular symphysis during loading and unloading for each experiment. Data for each chewing side (left or right) are not combined in order to determine if there is a chewing side effect on the strain patterns, particularly with respect to the direction of ε_1. The grand means reported here for left and right chews are calculated from these experimental means. The largest single peak maximum and minimum principal strain at loading, peak, and unloading from all experiments are also reported.

3.3 Results

3.3.1 Symphyseal Strains During in vitro Transverse Bending

During simulated wishboning of the fresh alpaca jaw, all elements on gauges 1–5 (labial surface) and 7–8 (lingual surface) sensed compression (Fig. 3.2). Moreover, the B-element of each rosette, oriented perpendicular to the long axis of the symphysis, sensed greater levels of tension as compared to the A- and C-elements. On the other hand, the two single-elements, gauges 6 and 9, sensed tension. Gauge 9, located on the curved, vertically oriented surface of the symphysis and sensed greater tension than gauge 6, the most caudally placed lingual gauge. Thus, during wishboning, most of the symphysis is in compression with only the caudal portion of the symphysis sensing tension. During simulated reverse wishboning, the above pattern is reversed. That is, gauges 1 through 8 record tensile strains along the labial and lingual surfaces of the symphysis, whereas gauges 6 and 9 sensed compression. Based on these strain patterns, gauges 1 through 5, 7, and 8 are on one side of the neutral axis during transverse bending, and gauges 6 and 9 are on the other side (Fig. 3.3).

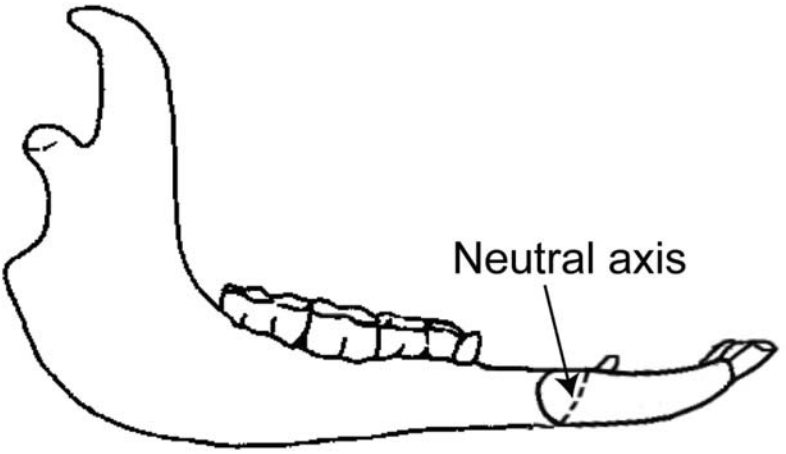

Fig. 3.3 Drawing of an alpaca mandible sectioned in the sagittal plane through the symphysis. The dashed line shows the approximate neutral axis during transverse bending as determined from the simulated loads and resulting strains presented in Fig. 3.2.

3.3.2 Symphyseal Strains During In Vivo Simulated Stresses and Mastication

3.3.2.1 Simulated Reverse Wishboning Strains

During simulated reverse wishboning, the maximum principal strain exceeds the minimum principal strain by a factor of 2–3.5 (Fig. 3.4). Moreover, the maximum principal strain is oriented between 90° and 105° relative to the long axis of the symphysis. The expected patterns of strain during medial and lateral transverse bending can be derived from the in vitro and in vivo strain data. During medial transverse bending, the maximum principal strain at the gauge site should be oriented at 90° relative to the long axis of the symphysis and about two to three times higher than the minimum principal strain (i.e., $\varepsilon_1/\varepsilon_2$should range from about 2.0–3.0) (Fig. 3.5). The opposite should occur during lateral transverse bending. Maximum principal strain at the gauge site should be oriented at 0° relative to the long axis of the symphysis, and principal compression should exceed principal tension. Theoretically, shifts in chewing side should have no effect on transverse bending strain patterns.

3.3.2.2 Overview of Masticatory Strains

In vivo masticatory strain data were collected from a total of five experiments on four animals. Alpaca 4 was used in two experiments. The animals vigorously chewed hay unilaterally on both the left and right sides in all but one experiment (Alpaca 2), yielding 315 left and 297 right analyzed chews. Raw and principal strains during a vigorous chewing bout by Alpaca 4 are presented in Fig. 3.6, along with associated information on jaw movements. There are two notable bouts of

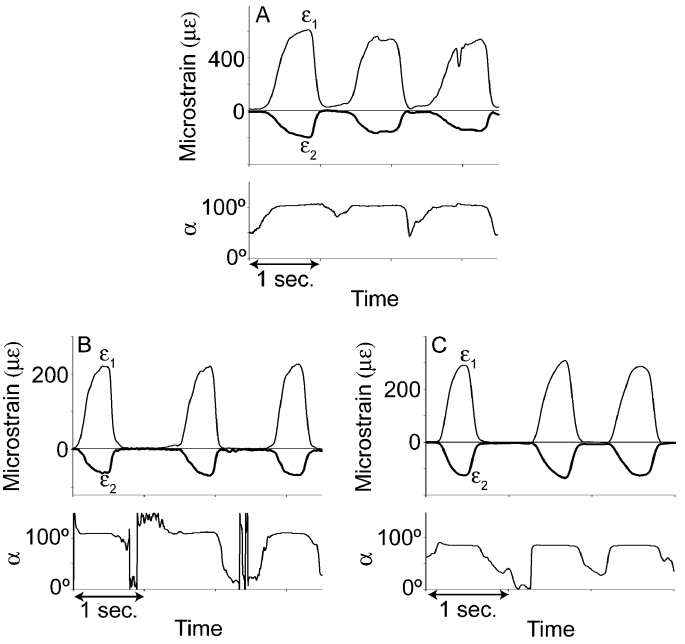

Fig. 3.4 Principal strains and the direction of maximum principal tension recorded from the symphyses of anesthetized alpacas during simulated manual reverse wishboning. (**A**) Alpaca 2 Experiment 1; (**B**) Alpaca 4 Experiment 1; (**C**) Alpaca 4 Experiment 2; ε_1, maximum principal strain (tension); ε_2, minimum principal strain (compression); α, direction of ε_1 relative to the A-element of the rosette and the long axis of the symphysis; sec., second

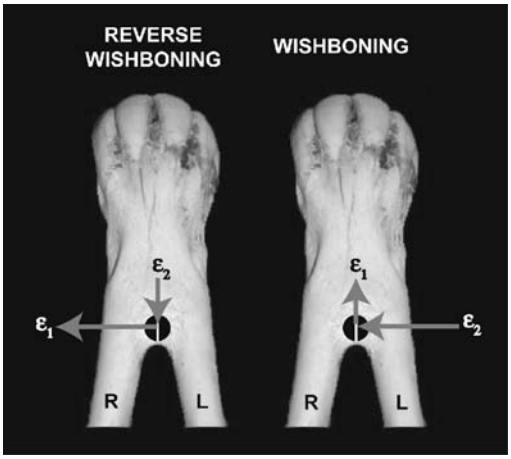

Fig. 3.5 Expected patterns of strain during reverse wishboning (i.e., medial transverse bending) and wishboning (i.e., lateral transverse bending) of the alpaca symphysis. The size of the arrow indicates the relative magnitude of the maximum and minimum principal strains (ε_1 and ε_2, respectively). The direction of ε_1 and ε_2 are determined relative to the A-element. All symbols as in previous figures

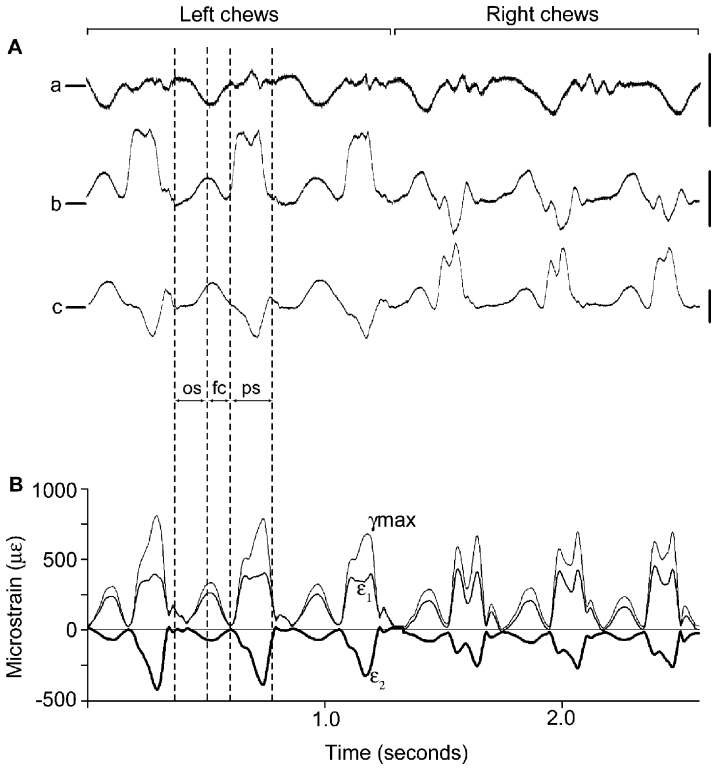

Fig. 3.6 Raw (**A**) and transformed (**B**) symphyseal strains during mastication by Alpaca 4 (Experiment 2). In **A**, raw strain traces from each of the gauge elements (a, b, and c) are shown. The 0 level of strain is shown by the horizontal bar next to each gauge-element label. Positive strains are tensile and negative strains are compressive. The scale bars to the right of each trace is 250 με. The opening stroke (os), fast-closing (fc), and the power stroke (ps) for one chewing cycle are indicated by the dashed vertical lines. In **B**, the principal (ε_1, ε_2) and shear (γmax) strains are shown

strains. During jaw opening, strains rise and peak at or near maximum gape. During fast-closing, strains decrease and subsequently increase again at the start of power stroke. Power stroke strains are complex, and there may be two to three minor peaks between which symphyseal strain does not fall to zero. Because the largest principal strains typically occur during the power stroke, we focus the remainder of this paper on strains during loading at 25% of peak γmax (25% loading), peak γmax, and unloading at 25% of peak γmax (25% unloading).

3.3.2.3 Summary Data of Principal Strains, $\varepsilon_1/\varepsilon_2$ and α at 25% Loading, Peak, and 25% Unloading

At 25% loading, the maximum and minimum principal strains average 101 με (s.d. = 52) and −25 με (s.d. = 33), respectively, for left-side chews (Table 3.1; Fig. 3.7). During right-side chews, ε_1 averages 85 με (s.d. = 48) and ε_2

Table 3.1 Summary data of symphyseal strains at 25% loading, peak, and 25% unloading of the power stroke of mastication

Chewing side	N	Total cycles	Phase	Maximum principal strain (ε_1)	Minimum principal strain (ε_2)	$\varepsilon_1/\varepsilon_2$	Direction of $\varepsilon_1(\alpha)$
			25% Load	101 ± 52	-25 ± 33	5.1 ± 5.0	$131^\circ \pm 16$
Left	5	315	Peak	308 ± 92	-155 ± 84	3.7 ± 4.2	$132^\circ \pm 14$
			25% Unload	96 ± 50	-28 ± 24	6.3 ± 6.7	$124^\circ \pm 34$
			25% Load	85 ± 48	-44 ± 9	2.1 ± 1.2	$46^\circ \pm 14$
Right	4	297	Peak	301 ± 138	-170 ± 64	1.9 ± 0.7	$48^\circ \pm 9$
			25% Unload	98 ± 41	-26 ± 25	4.8 ± 4.1	$51^\circ \pm 14$
Largest (side)			25% Load	195 (R)	−90 (L)	12.6 (L)	
			Peak	551 (L)	−439 (L)	11.2 (L)	
			25% Unload	212 (L)	−101 (L)	17.0 (L)	

N, total number of experiments across animals.

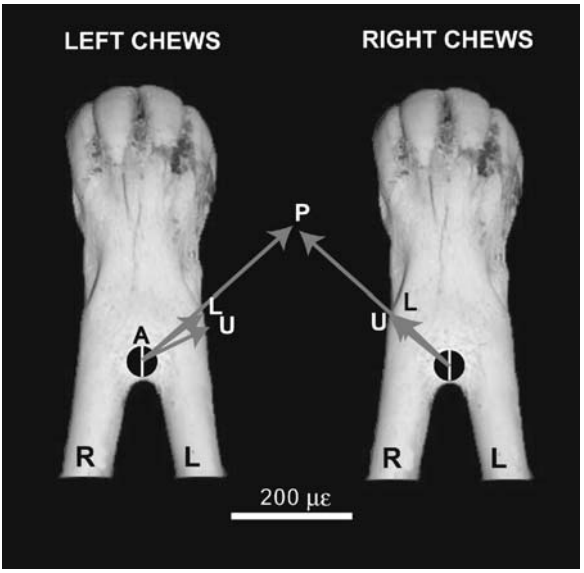

Fig. 3.7 Summary strain data from the symphysis of alpacas during left and right chews. Rt, right dentary; Lt, left dentary. The orientation of the A-element in each experiment is indicated by the white line on the gauge (*black circle*). Arrows indicate the magnitude and orientation of the maximum principal strains at 25% loading (L), peak (P), and 25% unloading (U)

averages $-44\,\mu\varepsilon$ (s.d. = 9). There is approximately a three- to fivefold increase in maximum principal strain magnitude from 25% loading to peak γmax, with ε_1 averaging $308\,\mu\varepsilon$ (s.d. = 92) and $301\,\mu\varepsilon$ (s.d. = 138) during left and right chews, respectively. The increase in minimum principal strain magnitude is slightly higher from 25% loading to peak, with left-side chews averaging $-155\,\mu\varepsilon$ (s.d. = 84) and right-side chews averaging $-170\,\mu\varepsilon$ (s.d. = 64). At 25% of peak γmax during unloading, ε_1 and ε_2 decrease to levels similar to those recorded at 25% loading. When chewing on the left, ε_1 averages $96\,\mu\varepsilon$ (s.d. = 50) and ε_2 averages $-28\,\mu\varepsilon$ (s.d. = 24). When chewing on the right, ε_1 averages $98\,\mu\varepsilon$ (s.d. = 41) and ε_2 averages $-26\,\mu\varepsilon$ (s.d. = 25).

The ratio of the principal strains (i.e., $\varepsilon_1/\varepsilon_2$) during all phases of the power stroke is greater than 1.0 for both left and right chews, indicating that the maximum principal strain exceeds the minimum principal strain (see Table 3.1). Principal strain magnitudes are most similar at peak γmax during both left and right chews as compared to at 25% loading and unloading. During left chews, $\varepsilon_1/\varepsilon_2$ averages 3.7 (s.d. = 4.2) whereas during right chews, $\varepsilon_1/\varepsilon_2$ averages 1.9 (s.d. = 0.7) at peak γmax. However, there is a significant amount of variation across experiments, with experimental means ranging from 1.0 to 12.6 at 25% loading, 1.1–11.2 at peak γmax, and 0.8–17.0 at 25% unloading.

The direction of ε_1 (i.e., α) varies as a function of chewing side in all experiments at each phase of jaw-closing (see Table 3.1; see Fig. 3.7). At 25% loading, α

averages 127° (s.d. = 15.3) when the animals chew on the left. When the animals chew on the right, α averages 53° (s.d. = 6.4). Thus, on average there is a 74° shift in the orientation of principal tension during loading. Mean angular data for ε_1 at peak γmax indicate that there is an 84° difference in the direction of tension along the symphysis between chewing sides. Maximum principal tension is oriented at 132° (s.d. = 14.0) and 48° (s.d. = 8.5) relative to the long axis of the symphysis during left- and right-side chews, respectively. At 25% unloading, this difference decreases to only 47°, with ε_1 oriented at 116° (s.d. = 26.7) during left-side chews and at 69° (s.d. = 27.2) during right-side chews.

Because α is determined relative to the A-element on the rosette, which is in line with the long-axis of the symphysis in the mid-sagittal plane, on average principal tension is oriented rostrally and to the left during left chews and rostrally and to the right during right chews (see Fig. 3.7). In the one experiment in which no right chews were recorded (Alpaca 2), the general orientation of principal tension during the left-side chews is similar to the other experiments at all phases of jaw-closing. Therefore, there probably would be a significant change in the orientation of principal tension if the animal had chewed on the right.

3.4 Discussion

3.4.1 Symphyseal Strains During Simulated Transverse Bending In Vitro and In Vivo: Implications for Interpreting Masticatory Strains

Based on the in vitro strains, expected strain patterns at the gauge sites associated with wishboning are straightforward: principal compression should exceed principal tension, and principal tension should be oriented at 0° relative to the long axis of the corpus. Chewing side should have no impact on the magnitude or orientation of principal strains during pure transverse bending.

The significance of the strain gradient along the lower border of the symphysis is less straightforward. Theoretically, the absolute value of the raw strains should increase at gauge sites farther from the neutral axis. However, according to the transverse bending simulation data on the alpaca jaw, strains from the B-element of each rosette on the upper and lower border of the symphysis tend to *decrease* rostrally. Therefore, if wishboning occurs during mastication, the recorded strains should be among the highest compressive strains along the labial aspect of the symphysis rather than the lowest. Of course, the largest strains along any portion of the symphysis will theoretically be tensile strains located along the caudal-most lingual margin during wishboning.

The above in vitro strain patterns associated with transverse bending could be the result of twisting moments introduced unintentionally during simulated transverse bending. An equally plausible explanation is that during transverse bending the alpaca symphysis does not behave as a curved beam being bent in its plane

of curvature. In addition to the external loads placed on the mandible, the shape and internal architecture of the symphysis influence strains along its outer surface. If the alpaca mandible does not behave as a curved beam during transverse bending, the identification of anteroposterior shear or transverse twisting from in vivo masticatory strain data is still possible. However, the identification of wishboning and medial transverse bending from masticatory strain data will not be as obvious without corresponding strain data from the same gauge site during simulated loading. More importantly, comparative analyses of symphyseal size and shape may not be sufficient for assessing relative wishboning resistance in camelid versus non-camelid selenodont artiodactyls (cf. Hogue and Ravosa, 2001).

3.4.2 Symphyseal Strains During Rhythmic Mastication

In alpacas, there appears to be two distinct phases of significant symphyseal loading during rhythmic mastication, one during jaw opening and the other during the power stroke. Although the jaw-opening strains were not analyzed in this study, a cursory review of the magnitude and orientation of the principal strains suggests that ε_1 typically exceeds ε_2 and ε_1 is oriented at 90° relative to the long axis of the corpus regardless of chewing side. This strain pattern is consistent with medial transverse bending of the symphysis as described above for the simulated stresses. Hylander (1984) found a similar pattern for jaw-opening strains in macaques.

Chewing side consistently influences the orientation of the principal strains during the power stroke. Regardless of the magnitude of the principal strains or the $\varepsilon_1/\varepsilon_2$ values, α differed by approximately 90° between left- and right-side chews at peak γmax and somewhat less during loading and unloading. Because the orientation of principal strains during left and right chews would be the same if the symphysis was bent transversely, symphyseal strain patterns are not consistent with wishboning. This does not mean that transverse bending does not occur. However, it does mean that it is not the predominant strain pattern during mastication.

According to Hylander (1984), there are several strain patterns that would show a 90° shift in the orientation of the maximum principal strain associated with changes in chewing side. These are dorsoventral shear, anteroposterior shear, and/or twisting about a transverse axis (Fig. 3.8). Dorsoventral shear is due to the upward vertical components of the muscle force on the balancing-side and the oppositely directed vertical components of the bite force on the working side (Hylander, 1984). The presence of this loading regime cannot be verified in alpacas because the symphysis is horizontally inclined, placing the gauge out of plane of the applied load (see Fig. 3.8). Moreover, as pointed out by Hogue and Ravosa (2001), the posteriorly placed masticatory muscles and relatively long jaws of selenodont artiodactyls are a mechanically unfavorable system for producing vertical bite force at the incisors, resulting in significantly reduced vertical reaction forces at the symphysis. Thus, while we cannot definitely rule out the presence of dorsoventral shear, it is unlikely that it would be a significant loading regime in alpacas. This is in contrast to

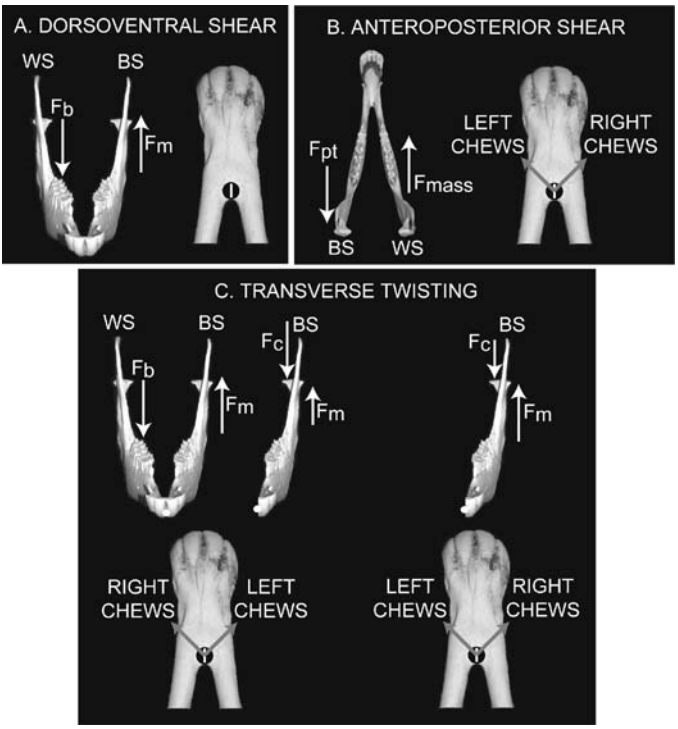

Fig. 3.8 Theoretical stresses and their expected patterns of strain during dorsoventral shear (**A**), anteroposterior shear (**B**), and transverse twisting (**C**) of the symphysis. WS, working side; BS balancing side; F_{pt}; F_{mass}; F_m, muscle force; F_b, bite force; F_c, condylar reaction force. White arrows indicate only the direction of the force. Gray arrows indicate the expected orientation of the maximum principal strain (ε_1) during left and right chews for each of the three loading regimes. Expected patterns of strain are indicated for the gauge site used in the in vivo experiments. During dorsoventral shear, there is no expected strain pattern because the gauge is out of plane of the applied load. See text and Hylander (1984) for additional details

macaques in which dorsoventral shear is a significant component of symphyseal loading during the power stroke (Hylander, 1984, 1985).

In contrast to dorsoventral shear, the gauges are aligned parallel to the shearing force due to anteroposterior shear. Anteroposterior shear of the symphysis was first described by Beecher (1977), who noted that when some mammals chew, the working-side dentary is displaced anteriorly relative to the balancing-side dentary during the power stroke. He hypothesized that this was due to the posteriorly directed pull of the balancing-side temporalis and the anteriorly directed pull of the working-side masticatory force. There are several reasons to conclude that the strain data do not reflect this loading regime either. If anteroposterior shear is the predominant loading regime, ε_1 would be directed at 45° during left-side chews and ε_1 and at 135° during right-side chews (see Fig. 3.8) (Hylander, 1984). The data presented above are directly opposite to this predicted pattern and, therefore,

anteroposterior shear is likely not the predominant loading regime during the power stroke along the alpaca symphysis.

The strain data are most consistent with transverse twisting of the symphysis. Transverse twisting of the symphysis is thought to be the result of the oppositely directed vertical components of the muscle force, bite force, and/or condylar reaction forces from the two sides of the jaw (see Fig. 3.8). However, the expected patterns of strain associated with transverse twisting are dependent on the combination of forces involved. For example, if twisting is a result of the vertical components of the bite force directed downward on the working side and the muscle force directed upward on the balancing side, the working-side corpus should be depressed and the balancing-side corpus should be elevated. For left-sided chews, the pattern of strain along the lower border of the labial aspect of the symphysis should indicate ε_1 directed at 45°, and during chews on the right side, ε_1 should be directed at 135° (Hylander, 1984). On the other hand, if transverse twisting results from the oppositely directed vertical components of the muscle force and condylar reaction force on the same side of the jaw, then the magnitude of the moments associated with these forces need to be considered. If the moment associated with the balancing-side condylar reaction force is larger than that of the balancing-side muscle force, then the balancing-side corpus will rotate in a counter-clockwise direction about the twisting axis of neutrality through the symphysis. This will result in ε_1 directed at 135° for chews on the left side and 45° for chews on the right side. If the moment associated with the balancing-side condylar reaction force is smaller than that of the bite force, then the balancing-side corpus will be rotated clockwise about the twisting axis of neutrality and the opposite strain pattern should occur. That is, ε_1 should be directed at 45° for left-side chews and 135° for right-side chews (see Fig. 3.8) (Hylander, 1984).

According to the strain data, the mandibular symphysis of alpacas is twisted about a transverse axis as due to the vertical components of the bite force on the working side depressing the corpus and those from the balancing-side muscles elevating the balancing-side corpus or from the vertical components of the balancing-side muscle force and oppositely directed balancing-side condylar reaction force. If this latter explanation is the case, then the moment associated with the condylar reaction force is larger than the moment associated with the balancing-side muscle force (see Fig. 3.8). This type of transverse twisting is similar to what has been observed in macaques (Hylander, 1984, 1985).

Although there is strong evidence in favor of transverse twisting of the symphysis, symphyseal strains reflect a combination of loading regimes because the maximum principal strains are rarely exactly at 45° and 135° during the power stroke and because principal strain magnitudes are not always equal. Deviations from this predicted pattern are most notable at 25% loading and 25% unloading, but they are also evident at peak loading. During loading and unloading, the ratio of the principal strains is on average higher than at peak loading and the orientation of ε_1 tends to be more transversely oriented across the symphysis, i.e., $\alpha > 45$ for right chews and $\alpha < 135$ for left chews. These patterns are consistent with frontal bending of the symphysis in which the labial aspect of the symphysis is loaded in tension and

the lingual aspect is loaded in compression. This may be due to the tendency of the mandibular corpora to twist about their long axes, inverting the alveolar process and everting the lower border (Hylander, 1984).

In summary, given the in vivo strain data, the alpaca symphysis is primarily twisted about a transverse axis upon which frontal bending may be superposed during portions of the closing phase of the chewing cycle.

3.4.3 Symphyseal Strains and Jaw Morphology in Alpacas

Based on the data presented above, there is little evidence for wishboning as the predominant masticatory loading regime of the alpaca symphysis. However, because strains were only quantified at peak γmax and at 25% of peak γmax during loading and unloading, it is unclear that these selected data points adequately characterize the complexity of symphyseal strains during the entire power stroke. Moreover, it is difficult to fully characterize what effect the late activity of the balancing-side deep masseter has on symphyseal strains when only these data points are considered. Therefore, a closer examination of the relationship between the late activity of the balancing-side deep masseter and symphyseal strains may shed some light on whether this jaw-muscle activity pattern can be directly tied to any component of masticatory strains along the symphysis.

Figure 3.9 provides an example of simultaneously recorded electromyographic and strain data from Alpaca 3 (Experiment 1). Of interest here is the second peak of balancing-side deep masseter activity, which appears to be correlated with a shift in the orientation and relative magnitude of the strains. During this time, principal compression slightly exceeds principal tension (i.e., $\varepsilon_1/\varepsilon_2 < 1.0$) and the orientation of ε_1 drops to around 0°, both of which are consistent with wishboning. In this particular chewing sequence, principal strains are typically negligible at less than 20 $\mu\varepsilon$. This second peak of balancing-side deep masseter activity is not always present across experiments or animals (Williams, 2004). However, when it does occur, it appears to affect symphyseal strains in the predicted manner, resulting in some noticeable but arguably negligible wishboning. The absence of wishboning associated with the first peak of balancing-side deep masseter activity (which is delayed relative to the other jaw adductors) is surprising, particularly given that these animals have strongly curved symphyses and a relatively long moment arm associated with wishboning. Perhaps, this laterally directed force exerted by the main burst of activity of the balancing-side deep masseter is resisted by a medially directed force from other muscles, such as the lateral pterygoid. Currently, we have no EMG data from alpacas to verify this hypothesis.

Given these results, can symphyseal strain patterns explain differences in symphyseal morphology between camelids and non-camelids? In order to answer this question, we undertook a broader consideration of symphyseal morphology in contrast to more traditional comparative biomechanical approaches that use beam theory to determine relative load resistance capabilities of the symphysis (e.g.,

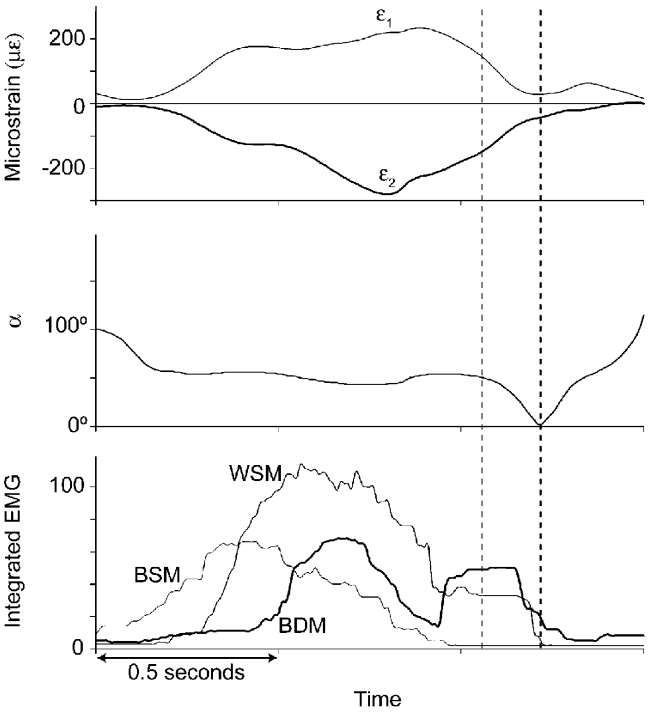

Fig. 3.9 Graphs showing the relationship between the principal strains (*top*), direction of $\varepsilon_1(\alpha)$ (*middle*) and integrated masseter EMG (*bottom*) from a single power stroke during chewing by an alpaca. BSM, balancing-side superficial masseter; BDM, balancing-side deep masseter; WSM, working-side superficial masseter. Dashed vertical lines through the graphs indicate the time at the end of the power stroke when strains indicate an increase in wishboning of the symphysis in association with a second peak of activity of the balancing-side deep masseter

Bouvier, 1986; Daegling, 1992, 2001; Daegling and Hylander, 1998; Hogue and Ravosa, 2001; Hylander, 1984, 1985; Ravosa, 1991, 1996a, b, 2000; Ravosa and Hogue, 2004; Vinyard and Ravosa, 1998; Vinyard et al., 2003; Williams et al., 2002). Following the classification system developed by Scapino (1981) for carnivorans, gross symphyseal morphology of unfused selenodont artiodactyls was examined using osteological specimens of two to five adult male and female individuals housed in the American Museum of Natural History. These observations highlighted the potential role that bony interdigitations in the symphysis can play in resisting the observed in vivo symphyseal loads. Bony interdigitations in the symphysis project from the surface of one dentary and fit into a corresponding depression in the symphyseal surface of the opposite dentary. Symphyses with relatively flat symphyseal surfaces are considered to be Class I symphyses whereas those that are fully fused are Class IV symphyses. Class II and Class III symphyses are both interdigitated, with Class III being the more heavily interdigitated.

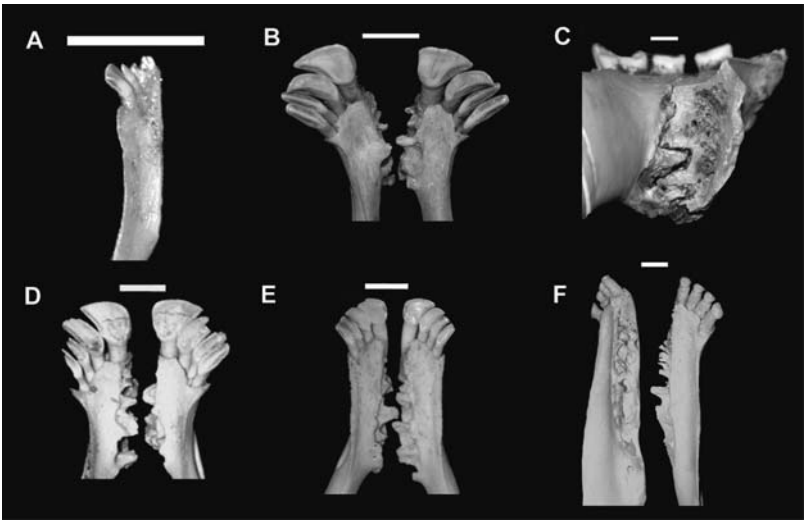

Fig. 3.10 Symphyses of four species of unfused selenodont artiodactyls: (**A**) *Tragulus javanicus*, Tragulidae; (**B**) *Procapra gutterosa*, Bovidae; (**C**) *Kobus ellipsiprymnus*, Bovidae; (**D**) *Dama dama*, Cervidae; (**E**) *Mazama mazama*, Cervidae; (**F**) *Okapi johnstoni*, Giraffidae. All scale bars are 1 cm. **A**, **B**, **D**, and **E** are lingual views. In **C**, the right dentary is broken through the symphyseal portion, exposing the interdigitating rugosities connecting the two hemimandibles. In **F**, the symphyseal plate of the left dentary is shown on the left and the lingual view of the right dentary is on the right. *Tragulus* is an example of a Class I symphysis. All other specimens are Class III symphyses

Of the 34 selenodont artiodactyl species examined, including representatives from all non-camelid extant families and 12 subfamilies, all but two species have Class III symphyses. The tragulids *Hyemoschus* and *Tragulus* have Class I symphyses (Fig. 3.10). In the species with Class III symphyses, the symphyseal plates are flatter in the region of the incisor roots where there are only minor interdigitations. Caudally, these interdigitations, which are offset both dorsoventrally and anteroposteriorly, typically increase in number and/or size throughout the symphysis. According to Lieberman and Crompton (2000), this is the region of the fibrocartilaginous pad in goats (see also Beecher, 1977, 1979; Scapino, 1981). Interestingly, examination of several infant and juvenile osteological specimens (e.g., *Ourebia ourebia, Antilocapra americana, Connochaetes gnou, Hippotragus equinus, Alcelaphus buselaphus*) indicates that they typically have relatively flat symphyseal surfaces (Class I), and the interdigitations become more pronounced with age in both number and size.

While these interdigitations increase the surface area for ligamentous attachment, they also help to resist forces loading the joint (Beecher, 1977; Lieberman and Crompton, 2000; Ravosa and Hylander, 1994; Rigler and Mlinsek, 1968; Scapino, 1981). Because they are interlocking and offset from one another in multiple vertical and anteroposterior planes, they can effectively resist anteroposterior shear, dorsoventral shear, and twisting of the symphysis about the transverse axis.

However, transverse twisting of the symphysis appears to be the dominant loading regime during the power stroke of mastication in alpacas. Thus, it is reasonable to assume that goats and other unfused selenodont artiodactyls also transversely twist their symphyses, for which symphyseal interdigitations in addition to ligaments and other connective tissues, likely provide some resistance.

These observations do not directly address the question of why camelids fuse their symphyses, particularly if all selenodont artiodactyls transversely twist their symphyses. A comparison on the mandibles of unfused and fused selenodont artiodactyls highlights one possible explanation linking symphyseal fusion to the strain data from alpacas, as well as taking into consideration the morphology of the unfused symphyses described above. In addition to fusion, camelids differ from unfused selenodont artiodactyls in having large, hypsodont, and deeply rooted incisors. Moreover, in contrast to unfused selenodont artiodactyls, the incisors of the South American camelids (alpaca, lama, vicuña, and guanaco) tend to radiate from the midline, leaving little room for a series of bony interdigitations. Finally, in young, pre-fused individuals, the incisors are very well developed at birth and it appears that they do not develop interdigitations prior to the initiation of fusion (Fig. 3.11).

Thus, based on the combined in vivo and morphological observations, we propose that selenodont artiodactyls will fuse if (1) they have to resist transverse twisting of the symphysis and (2) they have large, deeply rooted incisors precluding the accommodation of numerous deeply interdigitating rugosities. The link between incisor size and fusion has been proposed previously by other researchers including Greaves (1988) and Hiiemae and Kay (1972). However, in those hypotheses, symphyseal fusion is linked to incisor use during food procurement, for which there is very little behavioral data and no strain data. The hypothesis proposed here is the first to link relative incisor size, fusion, and symphyseal strains incurred during

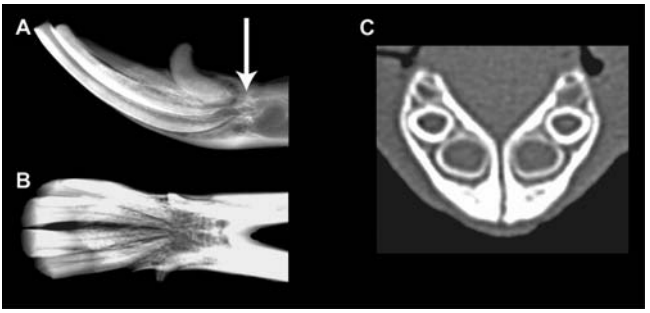

Fig. 3.11 The symphyseal region in South American camelids. (**A)** Lateral radiograph of the symphyses of an adult alpaca; (**B)** radiograph through the symphysis of a guanaco (*Lama guanicoe*); (**C)** computed tomography scan (sagittal plane) of the symphysis of a 4-month old alpaca. In **A**, the arrow indicates the caudalmost border of the symphysis in this specimen. Note the relatively large incisors and narrow symphyses in **A** and **B**. In the infant, the incisors are large and this region of the symphysis is unfused with flat symphyseal plates. The anterior 1/3 of the symphysis of this animal is already fused

mastication. Additional in vivo data as well as comparative data from extant and extinct camelids are currently being collected to evaluate this new hypothesis. Given the relatively robust experimental data set for cercopithecoid primates linking symphyseal fusion to wishboning, we stress that this hypothesis may only be applicable to selenodont artiodactyls.

3.5 Conclusions

Strain data from alpacas indicate that the symphysis is primarily twisted about a transverse axis during the power stroke of mastication. There is little evidence of wishboning at the levels of strain greater than 25% of peak strain. However, wishboning does occur toward the end of the power stroke at very minimal strain levels and is associated with the activity of the balancing-side deep masseter. While relative symphyseal dimensions in both primates and selenodont artiodactyls indicate that species with fused symphyses are better able to resist wishboning (Hogue and Ravosa, 2001; Hylander, 1985), the strain data from alpacas are not consistent with this biomechanical interpretation of mandibular form. Thus, whereas similar comparative studies in conjunction with in vivo data in primates coincide to offer a plausible explanation for fusion in anthropoids, biomechanical interpretations of symphyseal form and jaw-muscle activity patterns in selenodont artiodactyls are not necessarily indicative of symphyseal loading patterns (cf. Hogue and Ravosa, 2001; Williams et al., 2003).

Combined with the strain data, subsequent preliminary investigation into gross symphyseal morphology provides the foundation for a hypothesis linking fusion, incisor size, and the observed masticatory strains in selenodont artiodactyls. However, because additional data are required to more fully test this hypothesis, these observations should be treated as preliminary. Regardless, findings from this study suggest that while anthropoids and camelids may exhibit convergent and derived symphyseal morphologies as well as similarities in the firing patterns of their balancing-side deep masseters, there is likely more than one loading regime driving fusion of the symphysis in mammals. Moreover, unraveling its functional and adaptive significance will best be accomplished using multiple and complementary approaches including in vivo, in vitro, and comparative data.

Acknowledgments This chapter is based on a presentation given at the 74th Annual Meeting of the American Association of Physical Anthropologists in a symposium in honor of William L. Hylander. We would like to thank Dr. David Anderson, Head of Farm Animal Surgery and Director of the International Camelid Initiative, Department of Veterinary Clinical Sciences at The Ohio State University College of Veterinary Medicine, for the loan of the four alpacas used in this study. Many, many thanks go to the staff of the Duke University Department of Laboratory Animal Resources. We extend our thanks to Calvin Davis and Robert Parker of the Duke University Research Farm, who cared for the animals used in this study as well as assisted with animal handling during experiments. Kirk Johnson provided technical support during all phases of this project for which we are most grateful. Finally, we thank Eileen Westwig for facilitating the collection of data in the Division of Mammalogy in the American Museum of Natural History.

This research was supported by a National Science Foundation (NSF) Dissertation Improvement Grant (BCS-02-41652), grants from Sigma Xi and the Ford Foundation, as well as NSF research grants (BCS-01-38565 and IOS-05-020855).

References

Beecher, R.M. (1977). Function and fusion at the mandibular symphysis. *Am. J. Phys. Anthropol.* 47:325–336.

Beecher, R.M. (1979). Functional significance of the mandibular symphysis. *J. Morphol.* 159:117–130.

Bouvier, M. (1986). Biomechanical scaling of mandibular dimensions in New World Monkeys. *Int. J. Primatol.* 7:551–567.

Carter, D.R., Caler, W.E., Spengler, D.M., Frankel, V.H. (1981). Fatigue behavior of adult cortical bone: the influence of mean strain and strain range. *Acta Orthop. Scand.* 52:481–490.

Carter, D.R., Spengler, D., Frankel, V.H. (1977). Bone fatigue in uniaxial loading at physiologic strain rates. *IRCS Med. Sci.* 5:592.

Daegling, D.J. (1992). Mandibular morphology and diet in the genus *Cebus*. *Int. J. Primatol.* 13:545–570.

Daegling, D.J. (2001). Biomechanical scaling of the hominoid mandibular symphysis. *J. Morphol.* 250:12–23.

Daegling, D.J., Hylander, W.L. (1998). Biomechanics of torsion in the human mandible. *Am. J. Phys. Anthropol.* 105:73–87.

Greaves, W.S. (1988). A functional consequence of an ossified mandibular symphysis. *Am. J. Phys. Anthropol.* 77:53–56.

Hiiemae, K., Kay, R.F. (1972). Trends in the evolution of primate mastication. *Nature* 240:486–487.

Hogue, A.S., Ravosa, M.J. (2001). Transverse masticatory movements, occlusal orientation, and symphyseal fusion in selenodont artiodactyls. *J. Morphol.* 249:221–241.

Hylander, W.L. (1977). *In vivo* bone strain in the mandible of *Galago crassicaudatus*. *Am. J. Phys. Anthropol.* 46:309–326.

Hylander, W.L. (1979a). Functional significance of primate mandibular form. *J. Morphol.* 160:223–240.

Hylander, W.L. (1979b). Mandibular function in *Galago crassicaudatus* and *Macaca fascicularis*: an in-vivo approach to stress analysis of the mandible. *J. Morphol.* 159:253–296.

Hylander, W.L. (1984). Stress and strain in the mandibular symphysis of primates: a test of competing hypotheses. *Am. J. Phys. Anthropol.* 64:1–46.

Hylander, W.L. (1985). Mandibular function and biomechanical stress and scaling. *Am. Zool.* 25:315–330.

Hylander, W.L., Johnson, K.R. (1994). Jaw muscle function and wishboning of the mandible during mastication in macaques and baboons. *Am. J. Phys. Anthropol.* 94:523–547.

Hylander, W.L., Johnson, K.R., Crompton, A.W. (1987). Loading patterns and jaw movements during mastication in *Macaca fascicularis*: a bone-strain, electromyographic, and cineradiographic analysis. *Am. J. Phys. Anthropol.* 72:287–314.

Hylander, W.L., Ravosa, M.J., Ross, C.F., Wall, C.E., Johnson, K.R. (2000). Symphyseal fusion and jaw-adductor muscle force: an EMG study. *Am. J. Phys. Anthropol.* 112:469–492.

Hylander, W.L., Vinyard, C.J., Wall, C.E., Williams, S.H., Johnson, K.R. (2002). Recruitment and firing patterns of jaw muscles during mastication in ring-tailed lemurs. *Am. J. Phys. Anthropol. Suppl.* 34:88.

Hylander, W.L., Vinyard, C.J., Wall, C.E., Williams, S.H., Johnson, K.R. (2003). Convergence of the "wishboning" jaw-muscle activity pattern in anthropoids and strepsirrhines: the recruitment and firing of jaw muscles in *Propithecus verreauxi*. *Am. J. Phys. Anthropol. Suppl.* 36:120.

Hylander, W.L., Wall, C.E., Vinyard, C.E., Ross, C.F., Ravosa, M.J. (2004). Jaw adductor force and symphyseal fusion. In: Anapol, F., German, R.Z., Jablonski, N.G. (eds.), *Shaping Primate Evolution: Papers in Honor of Charles Oxnard*. Cambridge University Press, Cambridge, pp. 229–257.

Keaveny, T., Hayes, W. (1993). Mechanical properties of cortical and trabecular bone. In: Hall, B.K. (ed.), *Bone Growth*. CRC Press, Boca Raton, pp. 285–344.

Lieberman, D.E., Crompton, A.W. (2000). Why fuse the mandibular symphysis? A comparative analysis. *Am. J. Phys. Anthropol.* 112:517–540.

Luschei, E.S., Goodwin, G.M. (1974). Patterns of mandibular movement and jaw muscle activity during mastication in the monkey. *J. Neurophysiol.* 37:954–966.

Mama, K. (2000). Anesthetic management of camelids. In: Steffey, E.P. (ed.), *Recent Advances in Anesthetic Management of Large Domestic Animals*. International Veterinary Information Service, Ithaca (September 4, 2000; http://www.ivis.org/advances/Steffey_Anesthesia/mama_camelids/chapter_frm.asp?LA=1).

Ravosa, M.J. (1991). Structural allometry of the prosimian mandibular corpus and symphysis. *J. Hum. Evol.* 20:3–20.

Ravosa, M.J. (1996a). Jaw morphology and function in living and fossil Old World monkeys. *Int. J. Primatol.* 1996:909–932.

Ravosa, M.J. (1996b). Mandibular form and function in North American and European Adapidae and Omomyidae. *J. Morphol.* 229:171–190.

Ravosa, M.J. (1999). Anthropoid origins and the modern symphysis. *Folia Primatol.* 70:65–78.

Ravosa, M.J. (2000). Size and scaling in the mandible of living and extinct apes. *Folia Primatol.* 71:305–322.

Ravosa, M.J., Hogue, A.S. (2004). Function and fusion of the mandibular symphysis in mammals: a comparative and experimental perspective. In: Ross, C.F. Kay, R.K. (eds.), *Anthropoid Origins: New Visions*. Kluwer Press/Plenum Publishers, New York, pp. 399–488.

Ravosa, M.J., Hylander, W.L. (1994). Function and fusion of the mandibular symphysis in primates: stiffness or strength? In: Fleagle, J.G. Kay, R.F. (eds.), *Anthropoid Origins*. Plenum Press, New York, pp. 447–468.

Ravosa, M.J., Simons, E.L. (1994). Mandibular growth and function in Archaeolemur. *Am. J. Phys. Anthropol.* 95:63–76.

Ravosa, M.J., Vinyard, C.J., Gagnon, M., Islam, S.A. (2000). Evolution of anthropoid jaw loading and kinematic patterns. *Am. J. Phys. Anthropol.* 112:493–516.

Rigler, L., Mlinsek, B. (1968). Die Symphyse der Mandibula beim Rinde. Ein Beitrag zur Kenntnis ihrer Struktur und Funktion. *Anato. Anz.* 122:293–314.

Scapino, R.P. (1981). Morphological investigation into the function of the jaw symphysis in carnivorans. *J. Morphol.* 167:339–375.

Vinyard, C.J., Ravosa, M.J. (1998). Ontogeny, function, and scaling of the mandibular symphysis in papionin primates. *J. Morphol.* 235:157–75.

Vinyard, C.J., Wall, C.E., Williams, S.H., Hylander, W.L. (2003). A comparative functional analysis of skull morphology of tree-gouging primates. *Am. J. Phys. Anthropol.* 120:153–170.

Vinyard, C.J., Wall, C.E., Williams, S.H., Johnson, K.R., Hylander, W.L. (2006). Masseter electromyography during chewing in ring-tailed lemurs (*Lemur catta*). *Am. J. Phys. Anthropol.* 130:85–95.

Vinyard, C.J., Williams, S.H., Wall, C.E., Johnson, K.R., Hylander, W.L. (2001). Deep masseter recruitment patterns during chewing in callitrichids. *Am. J. Phys. Anthropol. Suppl.* 32:156.

Williams, S.H. (2004). Mastication in selenodont artiodactyls: an *in vivo* study of masticatory form and function in goats and alpacas. Ph.D. Thesis, Duke University, Durham.

Williams, S.H., Vinyard, C.J., Wall, C.E., Hylander, W.L. (2003). Symphyseal fusion in ungulates and anthropoids: a case of functional convergence? *Am. J. Phys. Anthropol. Suppl.* 36:226.

Williams, S.H., Vinyard, C.J., Wall, C.E., Hylander, W.L. (2007). Masticatory motor patterns in ungulates: a quantitative assessment of jaw-muscle coordination in goats, alpacas and horses. *J. Exp. Zool. Part A: Ecol. Genet. Physiol.*, 307:226–240.

Williams, S.H., Wall, C.E., Vinyard, C.J., Hylander, W.L. (2002). A biomechanical analysis of skull form in gum-harvesting galagids. *Folia Primatol.* 73:197–209.